

Supporting Information

# **Ru Single Atoms on One-Dimensional CF@g-C<sub>3</sub>N<sub>4</sub> Hierarchy as Highly Stable Catalysts for Aqueous Levulinic Acid Hydrogenation**

Ying Yang <sup>1,\*</sup>, Suoying Zhang <sup>2</sup>, Lin Gu <sup>1</sup> and Shijie Hao <sup>1,\*</sup>

<sup>1</sup> State Key Laboratory of Heavy Oil Processing, China University of Petroleum, Changping, Beijing 102249, China

<sup>2</sup> Institution of Advanced Materials, Nanjing Tech University, Nanjing 211816, China

\* Correspondence: yyang@cup.edu.cn (Y.Y.); haoshijie@cup.edu.cn (S.H.); Tel.: +86-10-89734979 (Y.Y.)

**Table S1** The atom percentage and elemental analysis for different Ru-containing catalysts

Catalyst	Percentage of different				Ru loading <sup>b</sup> (wt%)	Ru loss <sup>b</sup> (ppm)
	elements <sup>a</sup> (at. %)					
	C	N	O	Ru		
CF@g-C <sub>3</sub> N <sub>4</sub> -Ru SAs	55	18	20	7	3.0	0.004
CF@g-C <sub>3</sub> N <sub>4</sub> -Ru NPs	51	28	10	11	1.3	0.016
g-C <sub>3</sub> N <sub>4</sub> -Ru	-	-	-	-	4.5	-
CF-Ru	-	-	-	-	4.1	-

<sup>a</sup>Estimated by XPS.

<sup>b</sup>Detected by ICP-OES analysis.

**Table S2** Textural properties of various Ru-containing catalysts

Catalyst	$S_{\text{BET}}^{\text{a}}$ ( $\text{m}^2 \text{g}^{-1}$ )	$V_{\text{p}}^{\text{b}}$ ( $\text{cm}^3 \text{g}^{-1}$ )	$d_{\text{meso}}^{\text{c}}$ (nm)	$V_{\text{micro}}^{\text{d}}$ ( $\text{cm}^3 \text{g}^{-1}$ )	$d_{\text{micro}}^{\text{e}}$ (nm)	$X_{\text{mesoporosity}}^{\text{f}}$ (%)
CF@g-C <sub>3</sub> N <sub>4</sub> -Ru SAs	380	0.57	3.7	0.161	0.52	71.9
CF@g-C <sub>3</sub> N <sub>4</sub> -Ru NPs	266	0.25	3.5	0.103	0.60,0.65	60.0
g-C <sub>3</sub> N <sub>4</sub> -Ru	16	0.09	-	0.007	-	-
CF-Ru	587	0.30	3.4	0.227	0.51,0.62	23.3
spent CF@g-C <sub>3</sub> N <sub>4</sub> -Ru SAs	267	0.219	2.4	-	-	-
spent CF@g-C <sub>3</sub> N <sub>4</sub> -Ru NPs	195	0.159	2.1	-	-	-

<sup>a</sup>The BET surface area was obtained from the adsorption branches in the relative pressure range of 0.05~0.29.

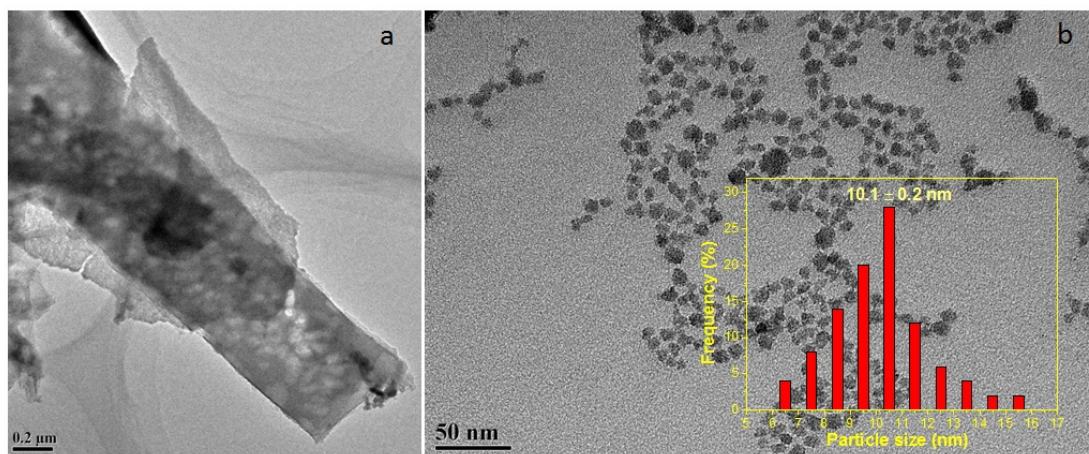
<sup>b</sup>The single point adsorption total pore volume was taken at the relative pressure of 0.99.

<sup>c</sup>The mesopore size distribution was calculated from the desorption branches by the Barret-Joyner-Halenda (BJH) method.

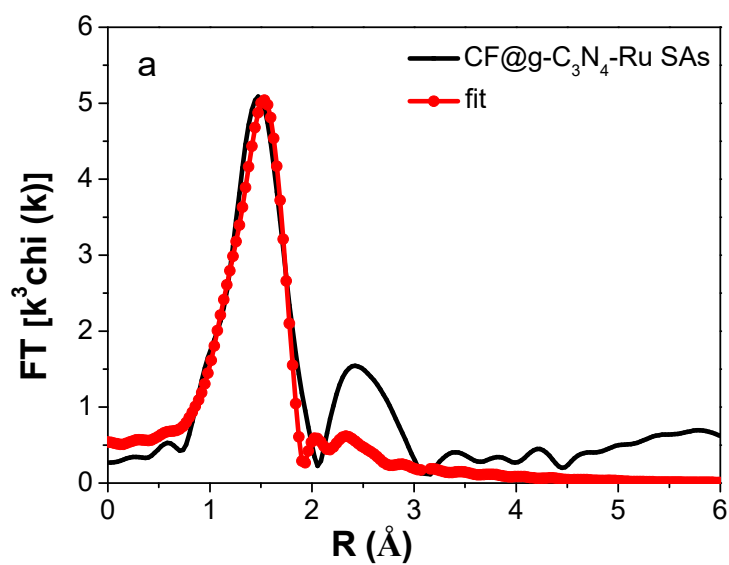
<sup>d</sup>The single point adsorption micropore volume was taken at the diameter less than 2 nm.

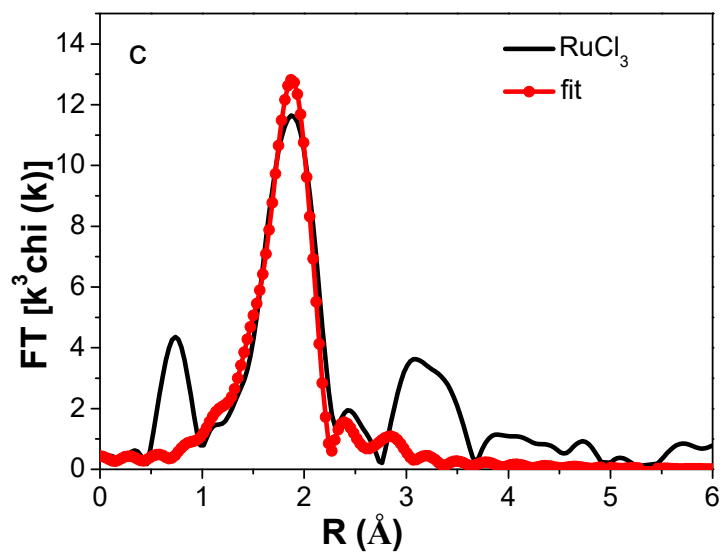
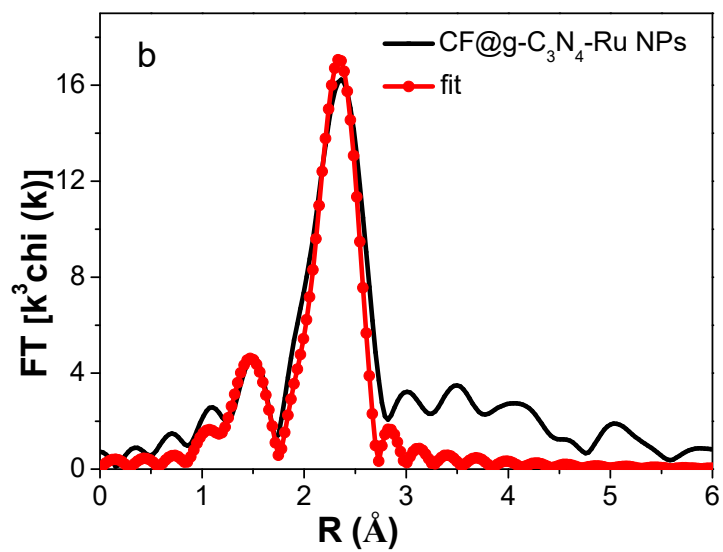
<sup>e</sup>The micropore size distribution was estimated by the Horvath-Kawazoe (H-K) method.

<sup>f</sup>The mesoporosity is defined as the ratio of  $V_{\text{meso}}/V_{\text{p}}$ , and was calculated according to the equation,  $X_{\text{mesoporosity}} = (1 - V_{\text{micro}}/V_{\text{p}}) \times 100\%$ .



**Figure S1.** TEM images for (a) CF@g-C<sub>3</sub>N<sub>4</sub>-Ru NPs and (b) filtrate obtained by ultrasonic treatment of CF@g-C<sub>3</sub>N<sub>4</sub>-Ru NPs in ethanol, with the corresponding particle size distribution histogram (inset).





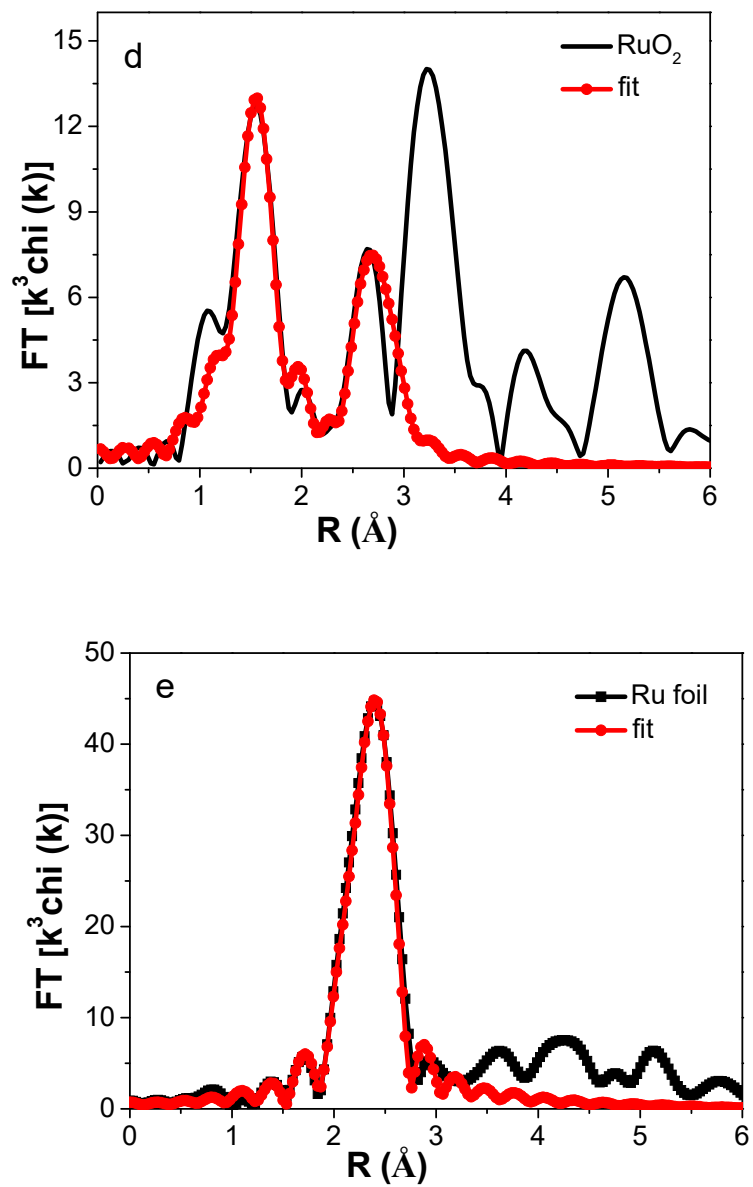


**Figure S2.** Curve fitting for (a) CF@g-C<sub>3</sub>N<sub>4</sub>-Ru SAs, (b) CF@g-C<sub>3</sub>N<sub>4</sub>-Ru NPs, (c) RuCl<sub>3</sub>, (d) RuO<sub>2</sub> and (e) Ru foil.

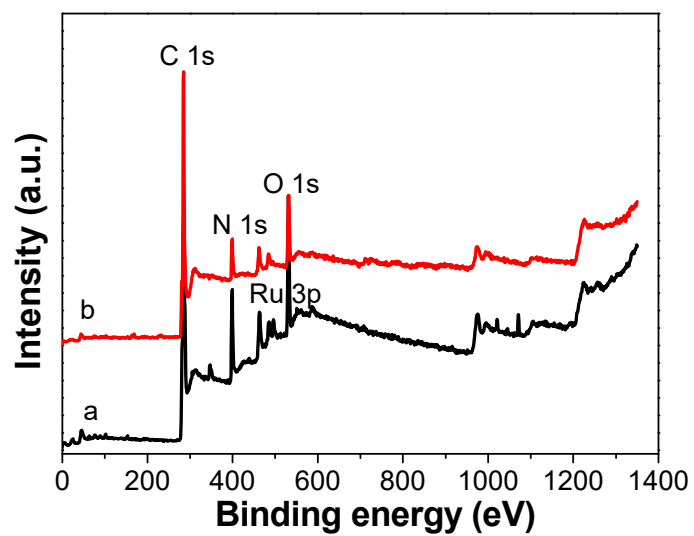


**Figure S3.** XPS survey scan for (a) CF@g-C<sub>3</sub>N<sub>4</sub>-Ru SAs and (b) CF@g-C<sub>3</sub>N<sub>4</sub>-Ru NPs.

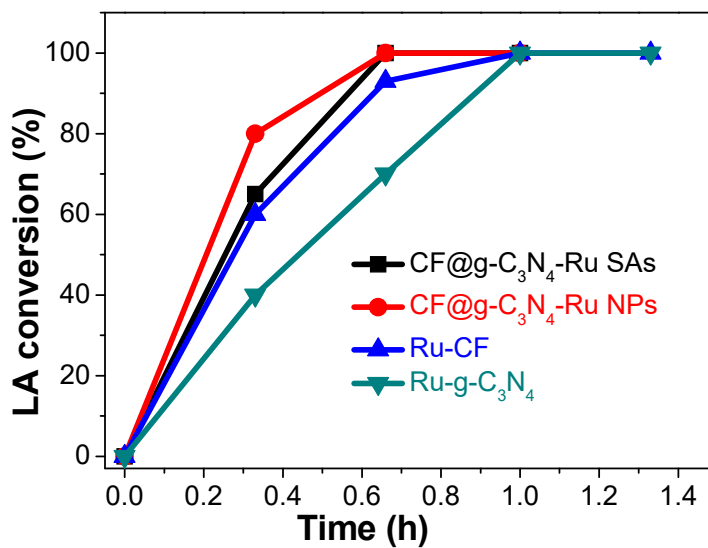


**Figure S4.** Time profiles for catalytic conversion of LA in water using different Ru-containing catalysts.

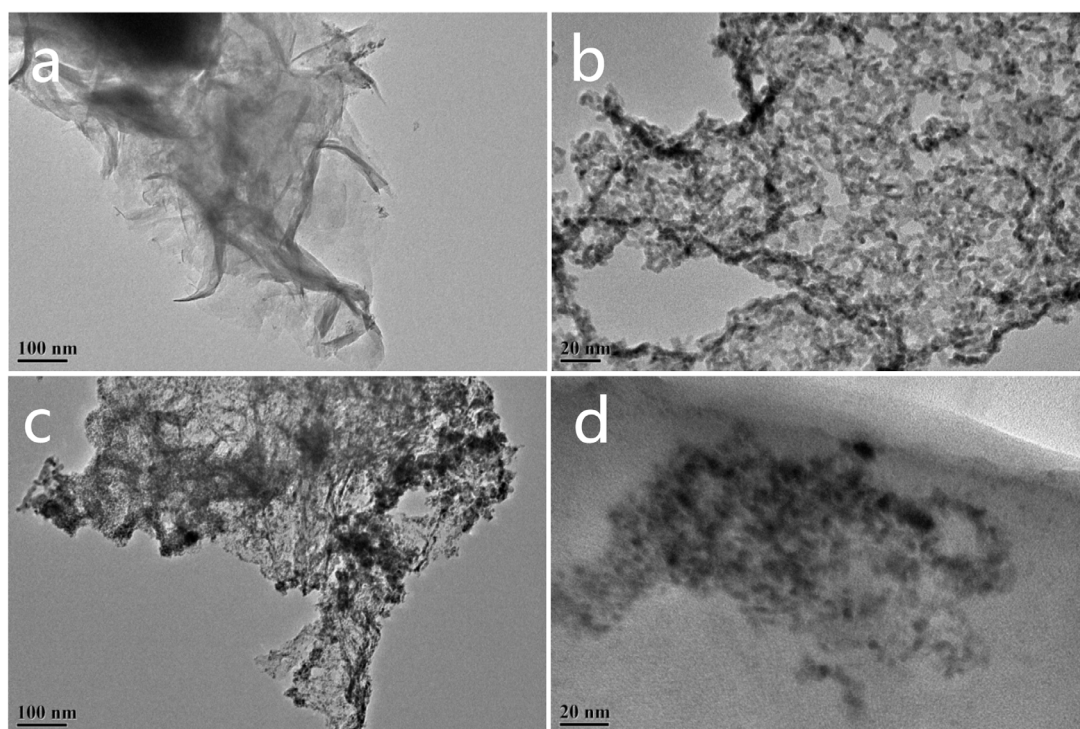


**Figure S5.** TEM images of (a,b) spent CF@g-C<sub>3</sub>N<sub>4</sub>-Ru SAs and (c,d) spent CF@g-C<sub>3</sub>N<sub>4</sub>-Ru NPs.

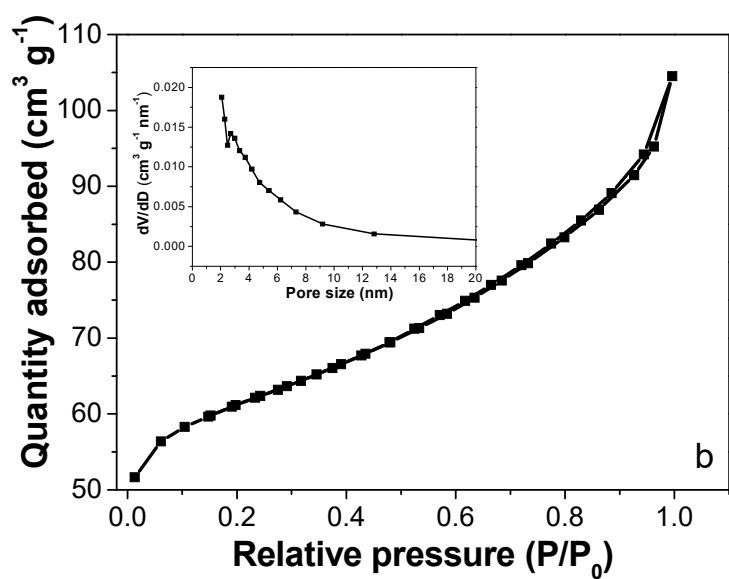
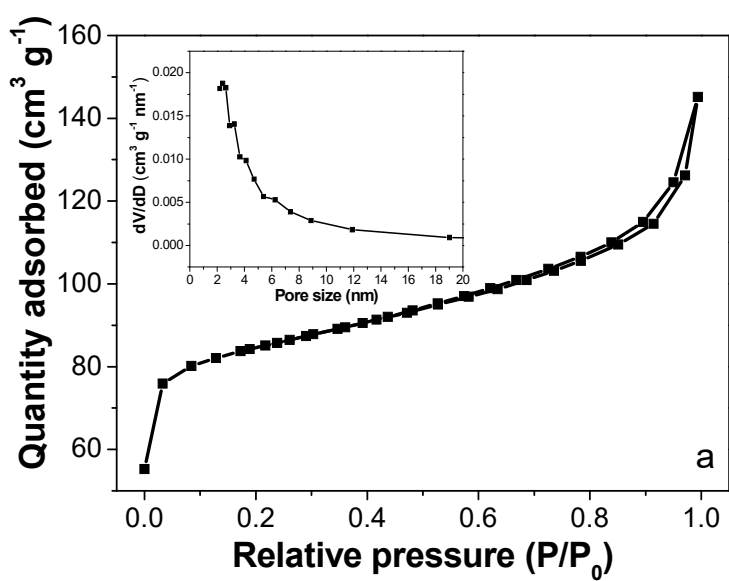


**Figure S6.** N<sub>2</sub> adsorption/desorption isotherm and the corresponding pore size distribution curve (inset) for (a) spent CF@g-C<sub>3</sub>N<sub>4</sub>-Ru SAs and (b) CF@g-C<sub>3</sub>N<sub>4</sub>-Ru NPs.

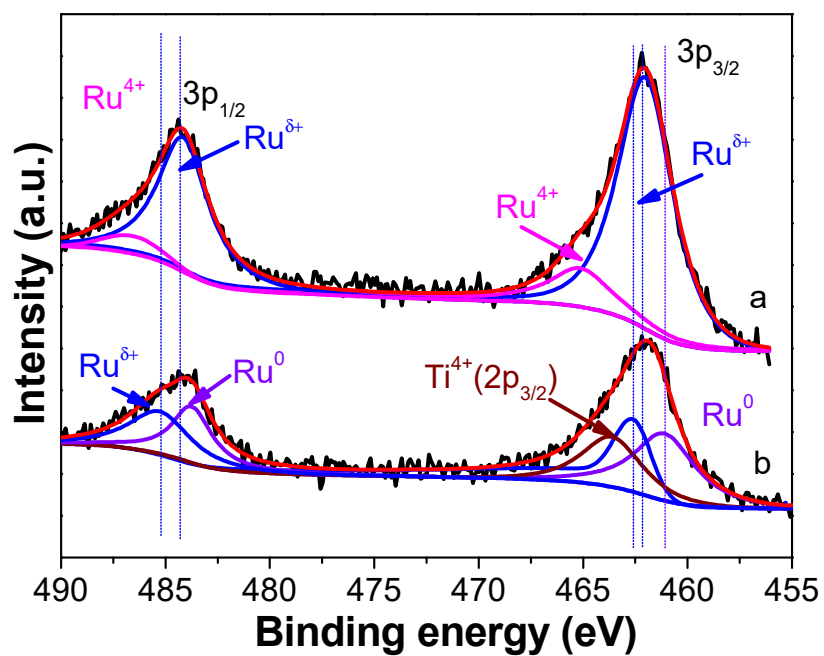


**Figure S7.** High-resolution Ru 3p spectra for (a) spent CF@g-C<sub>3</sub>N<sub>4</sub>-Ru SAs and (b) spent CF@g-C<sub>3</sub>N<sub>4</sub>-Ru NPs.